Neuroprediction of future rearrest

Eyal Aharoni[a,b,1,2], Gina M. Vincent[c], Carla L. Harenski[a], Vince D. Calhoun[a,d], Walter Sinnott-Armstrong[e], Michael S. Gazzaniga[f], and Kent A. Kiehl[a,b,2]

[a]Mind Research Network, Lovelace Biomedical and Environmental Research Institute, Albuquerque, NM 87106; Departments of [b]Psychology and [d]Electrical and Computer Engineering, University of New Mexico, Albuquerque, NM 87131; [c]Department of Psychiatry, University of Massachusetts Medical School, Worcester, MA 01604; [e]Department of Philosophy, and Kenan Institute for Ethics, Duke University, Durham, NC 27708; and [f]Department of Psychological and Brain Sciences, University of California, Santa Barbara, CA 93106

Identification of factors that predict recurrent antisocial behavior is integral to the social sciences, criminal justice procedures, and the effective treatment of high-risk individuals. Here we show that error-related brain activity elicited during performance of an inhibitory task prospectively predicted subsequent rearrest among adult offenders within 4 y of release ($N = 96$). The odds that an offender with relatively low anterior cingulate activity would be rearrested were approximately double that of an offender with high activity in this region, holding constant other observed risk factors. These results suggest a potential neurocognitive biomarker for persistent antisocial behavior.

impulsivity | recidivism | risk assessment

Risk assessment is a major component of criminal justice and treatment decisions. One crucial application of such predictions is the ability to identify, manage, and remediate antisocial behavior. Decisions that rely on antisocial risk prediction pervade the justice system, beginning with recommendations for bail, jail, and probation to sentencing, civil commitment, parole decisions, diversion, and treatment program assignments, to name a few. Initial attempts to predict future antisocial behavior based purely on clinicians' opinions have been shown to be highly inaccurate (1). Subsequent research that used evidence-based static (e.g., age, sex, criminal history) and dynamic (e.g., impulsivity, drug use, social support) risk factors have led to significant improvements in predicting future antisocial behavior (2–4).

One of the strongest and most widely studied risk factors for recidivism is impulsivity, or behavioral disinhibition, the persistent lack of restraint and consideration of consequences (3). Risk assessments, personality tests, and neuropsychological measures have been used to assess impulsivity and have demonstrated the ability to predict future antisocial behavior. However, these latter measures serve only as proxies for direct measurement of the brain's inhibitory and cognitive control systems. Indeed, neuroscientists have suggested that endophenotypes carry the potential to characterize underlying traits and abnormalities independently of behavioral phenotypes (5). This stance has been supported by recent functional MRI (fMRI) studies that have, for instance, accurately predicted choices in a motor-decision task (6), substance abuse relapse (7–10), and consumer purchases (i.e., neuromarketing) (11). These results raise the possibility that more direct measures of brain activity associated with impulse control may lend incremental utility to the prediction of future antisocial behavior.

The brain regions associated with impulse control have been well characterized. Consistent among these regions is the anterior cingulate cortex (ACC), a limbic region associated with error processing, conflict monitoring, response selection, and avoidance learning (12–16). Neurobiological models suggest that the ACC is central to an error-monitoring circuit wherein it relays error information from the basal ganglia and inferior frontal cortex to motor areas. These motor areas then update behavioral plans and feed back to the basal ganglia and frontal cortex, facilitating learning (12). Animal lesion studies have shown that focal damage to the anterior cingulate results in difficulty

learning to regulate behavior (17). In humans, cingulate damage has been shown to produce changes in disinhibition, apathy, and aggressiveness. Indeed, ACC-damaged patients have been classed in the "acquired psychopathic personality" genre (18). Moreover, engagement of the ACC during error conflicts in healthy adults has been shown to prospectively predict improvements in cognitive control (19).

Here we evaluate the hypothesis that ACC activity associated with a go/no-go (GNG) impulse control task will contribute to the prediction of future antisocial behavior (i.e., rearrest) in a longitudinal, prospective study of released criminal offenders. Several brain regions in addition to the ACC have been associated with impulse control (e.g., basal ganglia, dorsolateral prefrontal cortex). However, studies using Kiehl et al.'s (13) GNG task generally find the ACC is the most robustly engaged region during inhibitory control; thus we focus exclusively on the ACC region in this study.

Results

Association Between ACC and Error Rate. By using hierarchical linear regression, we examined the association between ACC response and the percentage of commission errors in the GNG task. As expected, lower ACC activity entered at step 2 corresponded to a higher rate of commission errors, controlling for variance attributable to age at step 1 ($R^2 = 0.08$, $\Delta R^2 = 0.04$, $\beta = -0.21$, $P < 0.05$). Mean commission error and hit rates on the GNG task were 25.04 (13.00) and 96.56 (6.40), respectively.

Survival Analysis. First, a Kaplan–Meier survival function was computed to describe the proportion of participants surviving any felony rearrest over the 4-y follow-up period, ignoring the influence of any particular risk factor (Fig. S1). Cox proportional-hazards regression was then used to examine (*i*) the zero-order effects of ACC activity on months to rearrest for any crime, (*ii*) the shared and unique influence of the ACC and other potential risk factors on months to rearrest for any crime, (*iii*) for nonviolent crimes, and (*iv*) the shared and unique influence of the medial prefrontal cortex (mPFC) control region and other potential risk factors on months to rearrest for any crime. Reliability of the β-coefficients was evaluated by resampling each Cox distribution in a bootstrapping sequence with 9,999 iterations.

Cox model A examined the zero-order effect of the error-related ACC response parameter on months to any felony rearrest before entering other covariates into the model (Tables 1

PSYCHOLOGICAL AND COGNITIVE SCIENCES

and 2). A significant association was found whereby, for every one unit increase in ACC activity, there was a 1.39 (i.e., 1/exp[B]) decrease in the probability of rearrest.

For the primary hypothesis test (model B), months to any felony rearrest was regressed on eight potential predictors including age, Hare Psychopathy Checklist–Revised (PCL-R) factor scores and their interaction, lifetime prevalence of alcohol or drug abuse or dependence, GNG commission error rate, and the ACC parameter (Tables 1 and 2). A significant effect of the overall model was obtained. Age and PCL-R factor 2 score exhibited marginal effects on rearrest with the use of a threshold of $P < 0.05$. The ACC was the only unique significant predictor that was robust to bootstrap resampling. For every one unit increase in ACC activity, there was a 1.96 (i.e., 1/exp[B]) decrease in the probability of rearrest ($P < 0.001$). For visualization purposes, this model was reconstructed with the use of a median split of "high" and "low" ACC activity (Fig. 1).

Model C was identical to model B except that the event criterion was defined as the presence of any nonviolent felony rearrest since release. Here, the predicted pattern of results was even more pronounced (Tables 1 and 2 and Fig. S2). A significant omnibus effect on rearrest was found. As earlier, this effect was driven by age, PCL-R factor 2, and ACC. For every one unit increase in ACC activity, there was a 2.44 decrease in the probability of rearrest after controlling for the other covariates ($P < 0.001$). As to be expected, the small number of participants rearrested for a violent offense ($n = 9$) was insufficient to justify an independent survival analysis of this group.

Model D was identical to model B except that the ACC parameter was replaced with that of an a priori control region (an anterior portion of the mPFC; see also ref. 5) not commonly implicated in response inhibition (Fig. S3). As expected, changes in mPFC activity were not associated with the probability of rearrest ($P = 0.20$).

Supporting analyses included individual Cox regressions for the seven observed risk factors (Table S1) and Pearson correlations (r) describing associations among all nine covariates (Table S2).

Discussion

The present analysis shows that hemodynamic activity within the brain prospectively predicted rearrest in an offender sample. The anatomical region associated with rearrest, the ACC, was defined by an a priori hypothesis related to response inhibition and error processing in healthy adults whereby increased ACC activity has been associated with improved inhibitory control (19). The ACC region demonstrated incremental predictive validity independent of other known risk factors and the GNG commission error rate, suggesting a possible predictive advantage over some behavioral and personality risk factors.

This pattern of results raises the possibility that brain activity in regions such as the ACC, elicited by a simple experimental task, may lend incremental utility to existing behavioral risk factors in the ability to predict rearrest. In addition, these results support existing theories that paralimbic function subserves the relationship between cognitive control and antisocial behavior (20) and that the ACC in particular may facilitate inhibitory learning by feeding error-related information to inhibitory control centers (12). Moreover, this pattern supports the view that neurocognitive endophenotypes carry the potential to characterize underlying traits and defects independently of behavioral phenotypes, such as self-report instruments and expert-rater diagnoses based on client interviews and collateral historical information. Finally, this work highlights potential neuronal systems that could be targeted for treatment intervention. One plausible hypothesis is that interventions that modulate ACC activity may help to increase cognitive control systems and thereby reduce future recidivism. Initial support for this hypothesis has already been reported in a recent study implicating the ACC in treatment responsiveness among children with externalizing problems (21).

Before sufficient confidence in the effects can be established, test–retest reliability must be demonstrated. Here, reliability of the ACC result was demonstrated by using bootstrap resampling. Release age and PCL-R factor 2 score also met this criterion, but only for nonviolent crimes. Additional research would be required to determine why the other covariates did not exhibit predictive effects. Efforts to replicate these results should examine the robustness to variations in task, sample characteristics, sample size, anatomical region of interest (ROI), and analytic procedures.

Should the neuroimaging effects be robust to replication, they remain silent on the question of suitability in making individual-level predictions. Whether neurobiological markers should ever be used to make predictions about individual offenders' risk is a thorny question that, at the least, depends on (i) whether these estimates can survive particular sensitivity and specificity thresholds with the use of large random samples, (ii) whether they can survive a required legal standard of proof, and (iii) whether their use would violate offender rights (22, 23). It is noteworthy that existing clinical risk assessment tools, including those reliant on personal health information about the offender, already permeate criminal justice decision settings, such as civil commitment decisions. We are skeptical that emerging neurobiological markers could ever independently outperform these existing tools in sensitivity and specificity, but they could potentially improve overall risk estimates in combination with known psychosocial risk factors. If so, their potential admissibility in legal settings may be greatest in decisions involving a low standard of proof such as treatment access decisions rather than in high-stakes decisions such as sentencing. However, even in low-stakes decisions, use of neurobiological information would force us to confront the question of whether it presents any unique civil rights challenges above and beyond that of existing practices (23). In this regard, one advantage that functional brain activity has vs. some other risk factors (e.g., age of first offense) is that the hemodynamic response is relatively dynamic, or amenable to change (24). Future treatment research efforts can potentially exploit this characteristic in the testing of therapies,

Table 1. Cox model statistics

Model	Description	−2 Log likelihood	Overall			Change from previous		
			χ^2	df	P value	$\Delta\chi^2$	df	P value
A	Any crime: zero-order	413.45	4.60	1	*	4.67	1	*
B	Any crime: ACC	327.65	17.35	8	*	18.33	8	*
C	Nonviolent crimes: ACC	244.33	25.48	8	**	28.43	8	***
D	Any crime: control region	337.77	8.27	8	0.41	8.21	8	0.41

Omnibus test of Cox regression model with χ^2 statistics showing (model A) the zero-order effect of ACC activity on months to rearrest for any crime, (model B) the shared and unique influence of the ACC and other potential risk factors on months to rearrest for any crime, (model C) for nonviolent crimes, and (model D) the shared and unique influence of the mPFC control region and other covariates on months to rearrest for any crime. *$P < 0.05$, **$P < 0.01$, and ***$P < 0.001$.

Table 2. Effect of individual predictors on rearrest

Model/predictor	B	SE (B)	Bootstrapped values B	SE(B)	P value	exp[B]	95% CI for exp[B]
Model A—zero-order: ACC							
ACC	−0.33	0.15	−0.33	0.14	*	0.72	0.53–0.97
Model B—any crime: ACC							
Age at release	−0.05	0.02	−0.05	0.03	0.07	0.96	0.91–1.00
PCL-R factor 1 score	−0.03	0.07	−0.03	0.09	0.73	0.97	0.85–1.11
PCL-R factor 2 score	−2.23	0.95	−2.23	1.34	0.06	0.11	0.02–0.70
PCL-R factor interaction	0.05	0.24	0.05	0.33	0.85	1.05	0.66–1.67
Alcohol abuse/dependence (lifetime)	0.08	0.20	0.08	0.24	0.72	1.08	0.72–1.61
Drug abuse/dependence (lifetime)	−0.31	0.37	−0.31	0.53	0.49	0.74	0.35–1.53
GNG commission error rate	−0.10	0.11	−0.10	0.15	0.41	0.90	0.73–1.12
ACC	−0.68	0.21	−0.68	0.23	***	0.51	0.34–0.76
Model C—nonviolent crimes: ACC							
Age at release	−0.07	0.03	−0.07	0.04	*	0.94	0.89–0.99
PCL-R factor 1 score	0.02	0.08	0.02	0.11	0.80	1.02	0.87–1.20
PCL-R factor 2 score	−3.68	1.16	−3.70	1.74	**	0.03	0.00–0.24
PCL-R factor interaction	0.36	0.33	0.36	0.45	0.31	1.43	0.76–2.72
Alcohol abuse/dependence (lifetime)	0.13	0.23	0.13	0.28	0.58	1.14	0.73–1.79
Drug abuse/dependence (lifetime)	−0.46	0.43	−0.46	0.66	0.37	0.63	0.27–1.45
GNG commission error rate	−0.06	0.13	−0.06	0.19	0.66	0.94	0.73–1.20
ACC	−0.88	0.24	−0.88	0.26	***	0.41	0.26–0.67
Model D—any crime: control region							
Age at release	−0.03	0.02	−0.03	0.03	0.19	0.97	0.93–1.01
PCL-R factor 1 score	−0.09	0.07	−0.09	0.08	0.19	0.91	0.80–1.04
PCL-R factor 2 score	−2.15	1.00	−2.15	1.31	0.07	0.12	0.02–0.83
PCL-R factor interaction	0.17	0.25	0.17	0.32	0.55	1.19	0.73–1.94
Alcohol abuse/dependence (lifetime)	−0.01	0.19	−0.02	0.21	0.93	0.99	0.68–1.43
Drug abuse/dependence (lifetime)	−0.01	0.38	0.00	0.52	0.99	0.99	0.47–2.10
GNG commission error rate	−0.01	0.11	0.00	0.13	0.96	0.99	0.80–1.23
mPFC	−0.15	0.11	−0.14	0.14	0.20	0.20	0.69–1.08

Results of Cox regression analyses examining the predictive effect of the ACC and other covariates on rearrest for (model A) any crime, (model B) any crime controlling for covariates, (model C) nonviolent crimes controlling for covariates, and (model D) the effect of the mPFC control region on rearrest for any crime controlling for covariates. Table reports unstandardized B, bootstrapped B, and relative risk ratio (exp[B]). *$P < 0.05$, **$P < 0.01$, and ***$P < 0.001$.

programs, and medications aimed at remediating problems in behavioral disinhibition. In the meantime, functional brain patterns may still be useful at the group level, enabling scientists to learn how certain cohorts with shared risk factors respond to different types of treatments to ultimately improve their access to early intervention options.

Methods

Participants. Participants were 96 adult male offenders ranging in age from 20 to 52 y (Mean, 33.1; SD, 7.78). Ten of them did not complete some of the assessments. Approximately 6% were left-hand–dominant. Based on National Institutes of Health racial and ethnic classification, 36% of the sample self-identified as white, 9% as black/African American, 9% as American Indian, 28% as mixed/OTHER, 42% as Hispanic, and 14% chose not to respond. They were paid $1/h, a rate commensurate with standard pay for work assignments at their facility.

Participants completed a number of psychological and behavioral assessment measures and an fMRI-based inhibition task using the Mind Research Network's Mobile MRI system before release from one of two New Mexico state correctional facilities. All participants were determined to be free of traumatic brain injury and psychosis, and had a general IQ of greater than 70. Participants reported having normal hearing, and visual acuity was normal or corrected to normal with the use of contact lenses or MRI-compatible glasses. After being released, they were tracked from 2007 to 2010. The average follow-up period was 34.5 mo. Participants provided written informed consent in protocols approved by the institutional review board of the University of New Mexico.

Nonoffender Sample. An independent sample of 102 healthy adult non-offenders (49 men) provided functional imaging results from which the a priori peak voxel could be defined. This sample was drawn from the Olin

Neuropsychiatry Research Center at the Institute of Living Hartford Hospital and the surrounding community of Hartford, CT, and ranged in age from 23 to 52 y (Mean, 33.92; SD, 9.64). Seven participants (7%) were left-handed. The sample reflected the ethnic nature of the community: 68% of the sample self-identified as white, 10% as black/African American, 9% as Hispanic, 8% as Asian, and 6% as mixed/other racial heritage.

Behavioral Task. Behavioral impulsivity was measured during fMRI using the GNG task, a widely used procedure that requires participants to inhibit a prepotent motor response. The task, modeled after the work of Kiehl et al. (13), presents participants with a frequently occurring target (the letter "X"; occurrence probability, 0.84) interleaved with a less-frequent distracter (the letter "K"; occurrence probability, 0.16) on a computer screen. Participants were instructed to depress a button with their right index finger as quickly and accurately as possible whenever they saw the target ("go" stimulus) and not when they saw the distractor ("no-go" stimulus). Because targets are more frequent than distracters in this task, a prepotent response toward the targets is elicited. When a distractor is presented, participants are required to inhibit their button response, which increases the rate of commission errors (Fig. S4). The commission error rate was defined as the proportion of observed commission errors among total no-go trials. Successful performance on this task requires the ability to monitor error-related conflicts and to selectively inhibit the prepotent go response on cue. Before scanning, participants completed a brief practice session of ~10 trials.

Experimental Design. The present fMRI study comprised an a priori ROI analysis, and all imaging data used for that ROI analysis are included in Dataset S1 in the form of a β-value for each subject. Dataset S1 also includes codes and scores from all other predictors and measures reported.

The experimental design was adopted from Kiehl et al. (13). Two scanning runs, each composed of 246 visual stimuli, were presented to
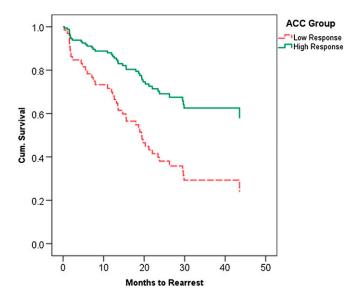
Fig. 1. Cox survival function showing proportional rearrest survival rates of high (solid green) vs. low (dashed red) ACC response groups for any crime over a 4-y period. Results of this median split analysis were equivalent to that of the parametric model: bootstrapped $B = 0.96$; SE = 0.40; $P < 0.01$; 95% CI, 0.29–1.84. The mean survival times to rearrest for the low and high ACC activity groups were 25.27 (2.80) mo and 32.42 (2.73) mo, respectively. The overall probabilities of rearrest were 60% for the low ACC group and 46% for the high ACC group.

participants using Presentation, a computer-controlled visual and auditory software (Neurobehavioral Systems). Stimuli were displayed on a rear-projection screen mounted at the rear entrance to the magnet bore and subtended a visual angle of ~3 × 3.5°. Each stimulus appeared for 250 ms in white text within a continuously displayed rectangular fixation box. Participants viewed the screen by means of a mirror system attached to the head coil.

The stimulus onset asynchrony (SOA) between go stimuli varied pseudorandomly among 1,000, 2,000, and 3,000 ms, subject to the constraint that three go stimuli were presented within each consecutive 6-s period. The no-go stimuli were interspersed among the go stimuli in a pseudorandom manner subject to three constraints: the minimum SOA between a go and a no-go stimulus was 1,000 ms; the SOA between successive no-go stimuli was in the range of 10 ± 15 s; and no-go stimuli had an equal likelihood of occurring at 0, 500, or 1,000 ms after the beginning of a 1.5-s acquisition period. By jittering stimulus presentation relative to the acquisition time, the

hemodynamic response to the stimuli of interest was sampled effectively at 500-ms intervals.

Behavioral responses were recorded by using a commercially available MRI-compatible fiberoptic response device (Lightwave Medical). Correct hits were defined as go (ie, X-stimuli) events that were followed by a button press within 1,000 ms of stimulus onset. Correct rejections were defined by an absence of a motor response within 1,000 ms of the no-go stimulus. Commission errors were defined as the presence of a response within 1,000 ms of the onset of a no-go stimulus.

Image Acquisition and Processing: Offender Sample. MRI acquisition parameters were identical to those of Harenski et al. (25). Images were collected with a mobile Siemens 1.5-T Avanto system with advanced SQ gradients (max slew rate, 200T/m/s; 346 T/m/s vector summation, rise time 200 µs) equipped with a 12-element head coil. The echoplanar image gradient-echo pulse sequence (repetition/echo times, 2,000/39 ms; flip angle, 75°; field of view, 24 × 24 cm; 64 × 64 matrix; 3.4 × 3.4-mm in-plane resolution; 5-mm slice thickness; 30 slices) effectively covers the entire brain (150 mm) in 2,000 ms. Head motion was limited by using padding and restraint. Functional images were reconstructed offline at 16-bit resolution and manually reoriented to approximately the anterior commissure/posterior commissure plane. Motion correction was achieved by using a preprocessing pipeline designed by Mazaika (26). Functional images were analyzed using Statistical Parametric Mapping software (SPM5). Functional images were spatially normalized to the Montreal Neurological Institute template via a nine-parameter affine transformation by using smooth basis functions to account for nonlinear differences (27), and spatially smoothed (8 mm full width at half maximum). High frequency noise was removed by using a low-pass filter (cutoff, 128s). Runs were normalized to an in-brain mean of 100 (arbitrary units) to compensate for intensity variations across runs [note that this is not the "proportional" scaling procedure that can result in artifactual deactivations when global effects are correlated with the local blood oxygen level-dependent (BOLD) signal] (28). Response types (hits and commission errors) were modeled as separate events. Event-related responses were modeled by using a synthetic hemodynamic response function composed of two γ-functions. The first γ-function modeled the hemodynamic response by using a peak latency of 6 s. A term proportional to the derivative of this γ-function was included to allow for small variations in peak latency. The second γ-function and associated derivative was used to model the small "overshoot" of the hemodynamic response on recovery. A latency variation amplitude-correction method was used to provide a more accurate estimate of hemodynamic response for each condition that controlled for differences between slices in timing and variation across regions in the latency of the hemodynamic response (29).

Functional images were computed for each participant that represented hemodynamic responses associated with commission errors and hits. Activity associated with these contrasts was evaluated in a whole-brain analysis across participants by using a t test in SPM5. All contrasts were corrected with a family-wise error (FWE) threshold of $P < 0.0001$ or higher
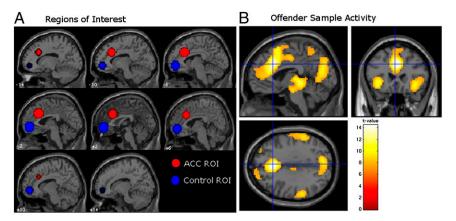

Fig. 2. (A) A priori seed region (red) for BOLD response to commission errors vs. correct hits in anterior cingulate from a GNG task with an independent sample of 102 healthy adult nonoffenders; peak voxel $x = -3$, $y = 24$, $z = 33$; radius = 14 mm sphere; $t(94) = 13.38$, $P < 0.0001$, FWE. A priori control region (blue) embodying anterior portion of the medial prefrontal cortex (peak voxel: 0, 51, −6; radius = 14 mm sphere). (B) Mean hemodynamic response change in offender sample ($n = 96$) during commission errors vs. correct hits from sagittal (*Upper Left*), coronal (*Right*), and axial (*Lower Left*) orientations. Peak activation located at $x = 3$, $y = 24$, $z = 33$ within the ACC ROI ($P < 0.00001$, FWE).

([Table S3](#)). Activations were overlaid on a representative high-resolution structural T1-weighted image from a single subject from the SPM5 canonical image set.

Image Acquisition and Processing: Nonoffender Sample. Imaging data were collected on a Siemens Allegra 3-T system located at the Olin Neuropsychiatry Research Center (Hartford, CT). The echoplanar image gradient-echo pulse sequence (repetition/echo times, 1,500/28 ms; flip angle, 65°) effectively covered the entire brain (150 mm) in 1.5 s. Functional image runs were motion-corrected by using an algorithm unbiased by local signal changes (INRIAlign) (30) as implemented in the SPM2 software (Wellcome Trust Centre for Neuroimaging, University College London). Normalized images were smoothed at 9 mm full width at half maximum. All other specifications were identical to that of the offender sample.

Functional ROIs. An a priori dorsal–caudal region of the ACC was developed from previous literature (13, 16, 31) (Fig. 2). This region has been associated with the "cognitive" as opposed to "affective" functions of the ACC (32). The seed coordinate was defined by the peak BOLD activity during commission errors vs. correct hits within an independent sample of 102 healthy adult nonoffenders who underwent the same GNG task (Fig. 1A). Defining hits as a baseline permitted the examination of commission errors while controlling for the motor response. A control region was also defined by this nonoffender dataset (a similar approach is described in ref. 5), namely an anterior portion of the mPFC, one of several regions that was not engaged by the GNG task in this nonoffender sample. Fourteen-millimeter radius spheres were defined around center coordinates derived from the activation peaks in each region. ROI activity was modeled by computing a mean β-value for each participant.

Covariate Risk Assessment. Data from several additional potential risk factors were obtained to examine the incremental predictive validity of the ACC response. All these variables have been previously found to predict antisocial behavior in offender populations or are correlated with activity within the anterior cingulate (19, 33). Indices of behavioral disinhibition included the commission error rates from the GNG task described earlier and scores from the Hare PCL-R (34), a detailed archival analysis and semistructured interview (Mean, 23.49; SD, 6.98). Twenty percent of the assessed sample (n = 90) met criteria for a diagnosis of psychopathy (score of ≥30). The PCL-R provides a reliable and valid assessment of psychopathy in incarcerated, forensic, psychiatric, and normal populations (35–37). To examine the independent clusters of psychopathic traits, the PCL-R items have also been organized into separable subfactors. The two-factor model distinguishes between interpersonal/affective attributes, such as glibness and lack of empathy, and antisocial behavioral attributes, such as early behavioral problems and impulsivity (factors 1 and 2, respectively). PCL-R total score was not entered into any models because of its collinearity with the entered PCL-R factor scores. Number of previous arrests was also not included as an independent predictor because this variable was part of the scoring criteria used on the assessment of PCL-R factor 2. PCL-R assessments were conducted by trained raters who exhibited high interrater reliability (intraclass correlation coefficient, 0.93) for the PCL-R total score (25).

Additional risk factors included age at release and lifetime prevalence of drug and alcohol abuse/dependence, which were assessed by using the structured clinical interview for the Diagnostic and Statistical Manual of Mental Disorders, Fourth Edition, Research Version (38). Abuse and dependence were defined by diagnostic scores of 2 and 3, respectively. Drug abuse/dependence included an average of scores from the following drug classes: sedatives, cannabis, stimulants, opioids, cocaine, and hallucinogens. Nine percent of the assessed sample (n = 92) qualified for drug abuse without dependence, and 87% qualified for drug dependence for at least one of the drug categories. Twenty-two percent qualified for alcohol abuse without dependence, and 58% qualified for alcohol dependence. Intelligence was assessed by using vocabulary and matrix reasoning subtests of the Wechsler Adult Intelligence Scale (Mean, 95.13; SD, 12.77) (39,40). [IQ is not typically a predictor of recidivism, but to ensure that IQ did not moderate the effect of the ACC in predicting rearrest, we conducted a supplementary survival analysis with IQ included in the model. In this model, the ACC still predicted rearrest whereas IQ did not. Model B (any crime): ACC, $B = -0.67$ (0.21), $P < 0.05$, exp[B] = 0.99 (95% CI, 0.96–1.01); IQ, $B = -0.02$ (0.02), $P = 0.67$, exp[B] = 0.99 (95% CI, 0.96–1.03). Model C (nonviolent crime): ACC, $B = -0.94$ (0.27), $P < 0.001$, exp[B] = 0.39 (95% CI, 0.23–0.66); IQ, $B = -0.01$ (0.02), $P = 0.67$, exp[B] = 0.99 (95% CI, 0.96–1.03).]

Follow-Up Procedure. Rearrest data, including arrest date and offense type, were obtained by a professional criminal background check service (SSC), which conducted national, state, and county criminal searches following each participant's release date. Approximately 53% of the sample was rearrested at least once between their release date (ranging from 2007 to 2010) and their follow-up date during July to September 2011. Offense type was classified into one of 27 common felony categories by 10 trained raters. In line with previous literature (41), minor parole and probation violations were excluded from analysis, and the remaining offenses were further classified as violent or nonviolent when warranted ([Table S4](#)). A larger portion of the sample was rearrested for nonviolent offenses (41.7%) than for violent offenses (9.4%).

Analytic Strategy. The primary hypothesis was evaluated by using Cox proportional-hazards regression. Cox regression is a semiparametric test that evaluates differences in individuals' time "at risk" to an event (e.g., rearrest) while estimating time for cases that have yet to reach that event (censored cases). The dependent variable is the cumulative survival function, or proportion of cases surviving the event. Hazard ratios (i.e., exp[B]) are computed to characterize each individual's relative odds of reaching the event for every one unit change in the risk factor (e.g., brain response), controlling for other covariates. All predictors were mean-centered.

1. Monahan JD (1981) *The Clinical Prediction of Violent Behavior* (Government Printing Office, Washington, DC).
2. Douglas KS, Webster CD, Hart SD, Eaves D, Ogloff JRP, eds (2001) *HCR-20: Violence Risk Management Companion Guide.* (Mental Health, Law, and Policy Institute, Simon Fraser University, Burnaby, BC, Canada).
3. Harris GT, Rice ME, Quinsey VL (1993) Violent recidivism of mentally disordered offenders: The development of a statistical prediction instrument. *Crim Justice Behav* 20(4):315–335.
4. Yang M, Wong SCP, Coid J (2010) The efficacy of violence prediction: A meta-analytic comparison of nine risk assessment tools. *Psychol Bull* 136(5):740–767.
5. Callicott JH, Weinberger DR (1999) Neuropsychiatric dynamics: The study of mental illness using functional magnetic resonance imaging. *Eur J Radiol* 30(2):95–104.
6. Soon CS, Brass M, Heinze HJ, Haynes JD (2008) Unconscious determinants of free decisions in the human brain. *Nat Neurosci* 11(5):543–545.
7. Janes AC, et al. (2010) Brain reactivity to smoking cues prior to smoking cessation predicts ability to maintain tobacco abstinence. *Biol Psychiatry* 67(8):722–729.
8. Sinha R, Li CS (2007) Imaging stress- and cue-induced drug and alcohol craving: Association with relapse and clinical implications. *Drug Alcohol Rev* 26(1):25–31.
9. Paulus MP, Tapert SF, Schuckit MA (2005) Neural activation patterns of methamphetamine-dependent subjects during decision making predict relapse. *Arch Gen Psychiatry* 62(7):761–768.
10. Camchong J, Stenger A, Fein G (2012) Resting-state synchrony during early alcohol abstinence can predict subsequent relapse. *Cereb Cortex*, 10.1093/cercor/bhs190.
11. Berns GS, Moore SE (2011) A neural predictor of cultural popularity. *J Consum Psychol* 22(1):154–160.
12. Holroyd CB, Coles MGH (2002) The neural basis of human error processing: Reinforcement learning, dopamine, and the error-related negativity. *Psychol Rev* 109(4): 679–709.
13. Kiehl KA, Liddle PF, Hopfinger JB (2000) Error processing and the rostral anterior cingulate: An event-related fMRI study. *Psychophysiology* 37(2):216–223.
14. Kosson DS, et al. (2006) The role of the amygdala and rostral anterior cingulate in encoding expected outcomes during learning. *Neuroimage* 29(4):1161–1172.
15. Mathalon DH, Whitfield SL, Ford JM (2003) Anatomy of an error: ERP and fMRI. *Biol Psychol* 64(1-2):119–141.
16. van Veen V, Carter CS (2002) The anterior cingulate as a conflict monitor: fMRI and ERP studies. *Physiol Behav* 77(4-5):477–482.
17. Gabriel M, Sparenborg SP, Kubota Y (1989) Anterior and medial thalamic lesions, discriminative avoidance learning, and cingulate cortical neuronal activity in rabbits. *Exp Brain Res* 76(2):441–457.
18. Devinsky O, Morrell MJ, Vogt BA (1995) Contributions of anterior cingulate cortex to behaviour. *Brain* 118(pt 1):279–306.

PSYCHOLOGICAL AND COGNITIVE SCIENCES

19. Kerns JG, et al. (2004) Anterior cingulate conflict monitoring and adjustments in control. *Science* 303(5660):1023–1026.
20. Kiehl KA (2006) A cognitive neuroscience perspective on psychopathy: Evidence for paralimbic system dysfunction. *Psychiatry Res* 142(2-3):107–128.
21. Woltering S, Granic I, Lamm C, Lewis MD (2011) Neural changes associated with treatment outcome in children with externalizing problems. *Biol Psychiatry* 70(9):873–879.
22. Faigman DL (2010) Evidentiary incommensurability: A preliminary exploration of the problem of reasoning from general scientific data to individualized legal decision-making. *Brooklyn Law Rev* 75:1115.
23. Nadelhoffer T, et al. (2010) Neuroprediction, violence, and the law: Setting the stage. *Neuroethics* 5:67–99.
24. Greely HT (2009) "Who knows what evil lurks in the hearts of men?": Behavioral genomics, neuroscience, criminal law, and the search for hidden knowledge. *The Impact of Behavioral Sciences on Criminal Law*, ed Farahani N (Oxford Univ Press, New York), pp 161–179.
25. Harenski CL, Harenski KA, Shane MS, Kiehl KA (2010) Aberrant neural processing of moral violations in criminal psychopaths. *J Abnorm Psychol* 119(4):863–874.
26. Mazaika P (2009) *Motion Correction and Despike Functions*. Available at http://cibsr.stanford.edu/documents/MotionandDespike.pdf. Accessed October 15, 2012.
27. Ashburner J, Friston KJ (1999) Spatial normalization. *Brain Warping*, ed Toga AW (Academic, New York) pp 27–44.
28. Desjardins AE, Kiehl KA, Liddle PF (2001) Removal of confounding effects of global signal in functional MRI analyses. *Neuroimage* 13(4):751–758.
29. Calhoun VD, Stevens MC, Pearlson GD, Kiehl KA (2004) fMRI analysis with the general linear model: Removal of latency-induced amplitude bias by incorporation of hemodynamic derivative terms. *Neuroimage* 22(1):252–257.
30. Freire L, Mangin JF (2001) Motion correction algorithms may create spurious brain activations in the absence of subject motion. *Neuroimage* 14(3):709–722.
31. Braver TS, Barch DM, Gray JR, Molfese DL, Snyder A (2001) Anterior cingulate cortex and response conflict: Effects of frequency, inhibition and errors. *Cereb Cortex* 11(9):825–836.
32. Bush G, Luu P, Posner MI (2000) Cognitive and emotional influences in anterior cingulate cortex. *Trends Cogn Sci* 4(6):215–222.
33. Monahan JD (2008) Structured risk assessment of violence. *Textbook of Violence Assessment and Management*, eds Simon R, Tardiff K (American Psychiatric Publishing, Washington, DC), pp 17–33.
34. Hare RD (2003) *Manual for the Hare Psychopathy Checklist-Revised* (Multi-Health Systems, Toronto), 3rd Ed.
35. Harpur TJ, Hare RD, Hakstian AR (1989) Two-factor conceptualization of psychopathy: Construct validity and assessment implications. *Psychol Assess* 1(1):6–17.
36. Hemphill JF, Hare RD, Wong S (1998) Psychopathy and recidivism: A review. *Leg Criminol Psychol* 3:141–172.
37. Fulero S (1995) Review of the Hare Psychopathy Checklist—revised. *Mental Measurements Yearbook*, eds Conoley JC, Impara JC (Buros Institute, Lincoln, NE) pp 453–454.
38. First MB, Spitzer RL, Gibbon M, Williams JBW (1997) *Structured Clinical Interview for DSM-IV Axis I Disorders – Clinical Version (SCID-IV)* (American Psychiatric Press, Washington, DC).
39. Wechsler D (1999) *Wechsler Adult Intelligence Scale* (Psychological Corporation, New York).
40. Ryan JJ, Lopez SJ, Werth TR (1999) Development and preliminary validation of a Satz-Mogel short form of the WAIS-III in a sample of persons with substance abuse disorders. *Int J Neurosci* 98(1-2):131–140.
41. Corrado RR, Vincent GM, Hart SD, Cohen IM (2004) Predictive validity of the Psychopathy Checklist: Youth Version for general and violent recidivism. *Behav Sci Law* 22(1):5–22.